

Contents lists available at [SciVerse ScienceDirect](http://www.sciencedirect.com)

## Biosensors and Bioelectronics

journal homepage: [www.elsevier.com/locate/bios](http://www.elsevier.com/locate/bios)

# Deep oxidation of glucose in enzymatic fuel cells through a synthetic enzymatic pathway containing a cascade of two thermostable dehydrogenases

Zhiguang Zhu<sup>a</sup>, Fangfang Sun<sup>a</sup>, Xiaozhou Zhang<sup>a,d</sup>, Y.-H. Percival Zhang<sup>a,b,c,d,\*</sup>

<sup>a</sup> Biological Systems Engineering Department, Virginia Polytechnic Institute and State University (Virginia Tech), 210-A Seitz Hall, Blacksburg, Virginia 24061, USA

<sup>b</sup> Institute for Critical Technology and Applied Science (ICTAS), Virginia Polytechnic Institute and State University, Blacksburg, Virginia 24061, USA

<sup>c</sup> DOE BioEnergy Science Center (BESC), Oak Ridge, Tennessee 37831, USA

<sup>d</sup> Gate Fuels Inc., 2200 Kraft Drive, Suite 1200B, Blacksburg, VA 24060, USA

## ARTICLE INFO

## Article history:

Received 12 January 2012

Received in revised form

26 March 2012

Accepted 4 April 2012

## Keywords:

Deep oxidation

Enzymatic fuel cell

Glucose biobattery

Thermoenzyme

Synthetic enzymatic pathway

## ABSTRACT

A synthetic enzymatic pathway was designed for the deep oxidation of glucose in enzymatic fuel cells (EFCs). Polyphosphate glucokinase converts glucose to glucose-6-phosphate using low-cost, stable polyphosphate rather than costly ATP. Two NAD-dependent dehydrogenases (glucose-6-phosphate dehydrogenase and 6-phosphogluconate dehydrogenase) that were immobilized on the bioanode were responsible for generating two NADH per glucose-6-phosphate (i.e., four electrons were generated per glucose *via* a diaphorase-vitamin K<sub>3</sub> electron shuttle system at the anode). Additionally, to prolong the enzyme lifetime and increase the power output, all of the recombinant enzymes that originated from thermophiles were expressed in *Escherichia coli* and purified to homogeneity. The maximum power density of the EFC with two dehydrogenases was 0.0203 mW cm<sup>-2</sup> in 10 mM glucose at room temperature, which was 32% higher than that of an EFC with one dehydrogenase, suggesting that the deep oxidation of glucose had occurred. When the temperature was increased to 50 °C, the maximum power density increased to 0.322 mW cm<sup>-2</sup>, which was approximately eight times higher than that based on mesophilic enzymes at the same temperature. Our results suggest that the deep oxidation of glucose could be achieved by using multiple dehydrogenases in synthetic cascade pathways and that high power output could be achieved by using thermostable enzymes at elevated temperatures.

© 2012 Elsevier B.V. All rights reserved.

## 1. Introduction

Enzymatic fuel cells (EFCs) usually utilize oxidoreductases as biocatalysts for generating electrical energy through the oxidation of chemical compounds at the anode (Cooney et al., 2008; Minteer et al., 2007). EFCs are receiving increasing interest as a next-generation, environmentally friendly, micro-power source because they could have high energy storage density, are safe and biodegradable, and utilize less costly enzymes (Cooney et al., 2008; Minteer et al., 2007). Unlike microbial fuel cells that use whole-cell microorganisms as biocatalysts, EFCs with potentially higher power outputs could have more applications because there are no cellular membranes to limit mass transfer and high enzyme loading can be achieved without the dilution effect of other biomacromolecules (Osman et al., 2011). To power portable electronic devices, there is an urgent need to increase the power density of EFCs, increase the

degree of fuel oxidation (i.e., increase energy storage density) and prolong the enzyme lifetime (Cooney et al., 2008; Davis and Higson, 2007; Minteer et al., 2007).

Glucose is the most common fuel used in EFCs because it is inexpensive, abundant, renewable, and safe (neither toxic nor corrosive) compared with methanol and ethanol (Zhang, 2011). To increase the power density of EFCs so that they will be suitable for numerous potential applications, intense efforts have been made to optimize factors such as enzyme selection, enzyme immobilization, electrode materials, and system configuration (Coman et al., 2010; Gao et al., 2009; Moehlenbrock et al., 2011; Sakai et al., 2009; Zebda et al., 2011). Recently, scientists at Sony demonstrated a glucose-powered EFC with a power density of 1.45 mW cm<sup>-2</sup> that uses one glucose dehydrogenase (Sakai et al., 2009). Furthermore, Cosnier and his coworkers developed a glucose oxidase-based EFC that produced 1.3 mW cm<sup>-2</sup> for more than one month at room temperature (Zebda et al., 2011). Most of them developed EFCs by using commercial mesophilic enzymes.

To increase the fuel utilization efficiency of EFCs, the deep oxidation of fuels mediated by enzyme cascades is highly desired (Sokic-Lazic et al., 2010; Zhang, 2010). Synthetic pathways containing

\* Corresponding author at: Biological Systems Engineering Department, Virginia Polytechnic Institute and State University (Virginia Tech), 304 Seitz Hall, Blacksburg, Virginia 24061, USA.

E-mail address: [ypzhang@vt.edu](mailto:ypzhang@vt.edu) (Y.-H.P. Zhang).

several oxidoreductases have been constructed to perform the complete or deep oxidation of methanol, ethanol, glycerol, and pyruvate (Akers et al., 2005; Arechederra et al., 2007; Palmore et al., 1998; Sokic-Lazic and Minteer, 2009). However, nearly all of the reported glucose-powered EFCs are based on the use of one oxidoreductase (i.e., glucose dehydrogenase or glucose oxidase), which results in the generation of only two electrons per glucose (Coman et al., 2010; Gao et al., 2009; Moehlenbrock et al., 2011; Sato et al., 2005; Zebda et al., 2011). Recently, Minteer et al. have demonstrated the use of a six-enzyme pathway at the anode surface that can oxidize glucose to  $\text{CO}_2$ , but its maximum power density was very low (i.e.,  $0.0065 \text{ mW cm}^{-2}$ ) (Xu and Minteer, 2011).

To prolong the enzyme lifetime in EFCs, most efforts have focused on the immobilization of commercially available enzymes, which usually originate from mesophilic organisms, on electrodes. Such immobilization not only prolongs the enzyme lifetime but also enhances electron transfer between the enzymes and electrodes (Moehlenbrock and Minteer, 2008; Rubenwolf et al., 2011). Typical methods of immobilization include simple adsorption, entrapment, wiring, covalent linking, and sandwiching (Zhang et al., 2011). The use of mesophilic enzymes might restrict the working temperature of EFCs to a narrow range. Alternatively, enzyme stability can be enhanced greatly through the utilization of thermoenzymes isolated from thermophiles (Wang et al., 2011) and protein engineering, such as rational design, directed evolution or a combination of these two strategies (Güven et al., 2010). However, the enzyme-oriented strategies have rarely been used by electrochemists.

In this study, a novel synthetic pathway was designed to perform the deep oxidation of glucose, i.e., the generation of four electrons per glucose (Fig. 1). Additionally, we investigated the feasibility of using recombinant thermostable enzymes for enhancing power densities at elevated temperatures.

## 2. Materials and methods

### 2.1. Materials

Chemicals, such as poly-L-lysine (PLL, MW  $\sim 70$ – $150$  kDa), vitamin  $\text{K}_3$  ( $\text{VK}_3$ ), polyacrylic acid sodium salt (PAAcNa, MW  $\sim 240$  kDa), and glucose-6-phosphate dehydrogenase (G6PDH) from *Leuconostoc mesenteroides*, were purchased from Sigma-Aldrich (St. Louis, MO, USA) unless stated otherwise. The polyphosphate (sodium

polyphosphate) that was used had an average degree of polymerization of 17. Phusion DNA polymerase from New England Biolabs (Ipswich, MA) was used for polymerase chain reaction (PCR). The carbon paper (AvCarb MGL200) that was used as the anode was purchased from Fuel Cell Earth (Stoneham, MA). Membrane electrode assemblies (MEAs), including Nafion 212 and the carbon cloth gas diffusion cathode coated with  $0.5 \text{ mg cm}^{-2}$  Pt, were purchased from Fuel Cell Store (San Diego, CA).

### 2.2. Cloning, expression and purification of recombinant thermoenzymes

The 1485-bp DNA fragment containing the open reading frame (ORF) of the glucose-6-phosphate dehydrogenase (*g6pdh*) gene (GenBank accession number JQ040549) was amplified by PCR from the genomic DNA of *Geobacillus stearothermophilus* 10 (Bacillus Genetic Stock Center accession number 9A21) using a pair of primers (forward primer: 5'-ACT TTA AGA AGG AGA TAT ACA TAT GAA CCC GAA ATC GAT CAT CGT CAT TT-3'; reverse primer: 5'-AGT GGT GGT GGT GGT GGT GCT CGA GCG AAC GCG GAT GCT CGA TCG GCC AC-3'). The vector backbone of pET20b was amplified by PCR using a pair of primers (forward primer: 5'-GTG GCC GAT CGA GCA TCC GCG TTC GCT CGA GCA CCA CCA CCA CCA CT-3'; reverse primer: 5'-AAA TGA CGA TGA TCG ATT TCG GGT TCA TAT GTA TAT CTC CTT CTT AAA GT-3'). The PCR products were purified using the Zymo Research DNA Clean & Concentrator Kit (Irvine, CA). With the newly developed restriction enzyme-free, ligase-free and sequence-independent Simple Cloning technique (You et al., 2012), the insertion fragment and vector backbone were assembled by prolonged overlap extension PCR, and the PCR product was directly transformed into *E. coli* TOP10 cells, yielding the chimeric plasmid pET20b-Gsg6pdh.

The 636-bp DNA fragment encoding diaphorase (DI, GenBank accession number JQ040550) was amplified by PCR using the genomic DNA of *G. stearothermophilus* 10 as the template and two primers (forward primer: 5'-ACT TTA AGA AGG AGA TAT ACA TAT GAC GAA AGT ATT GTA CAT CAC CGC CC-3'; reverse primer: 5'-AGT GGT GGT GGT GGT GGT GCT CGA GAA ACG TGT GCG CCA AGT CTT TCG CC-3'). The vector backbone of pET20b was amplified by PCR using the pET20b plasmid as the template and two primers (forward primer: 5'-GGC GAA AGA CTT GGC GCA CAC GTT TCT CGA GCA CCA CCA CCA CCA CT-3'; reverse primer: 5'-GGG CGG TGA TGT ACA ATA CTT TCG TCA TAT GTA TAT CTC CTT CTT AAA GT-3'). Plasmid pET20b-Gsdi was obtained using Simple Cloning (You et al., 2012) to express the recombinant GsDI (briefly called DI).

The recombinant plasmids were transformed into *E. coli* BL21 Star (DE3). Two hundred and fifty milliliters of LB medium supplemented with  $100 \mu\text{g mL}^{-1}$  of ampicillin in 1-L Erlenmeyer flasks was inoculated with the transformed *E. coli* cells and incubated at a rotary shaking rate of 220 rpm at  $37^\circ\text{C}$  until the  $A_{600}$  reached between  $\sim 0.6$  and  $0.8$ . The expression of the recombinant protein was induced by adding isopropyl  $\beta$ -D-1-thiogalactopyranoside (IPTG) ( $0.1 \text{ mM}$  final concentration). The cultures were then incubated at a decreased temperature of  $18^\circ\text{C}$  for 16 h. The cells were harvested by centrifugation at  $4^\circ\text{C}$ . The collected cells were disrupted by sonication, and the soluble target protein in the supernatant of the crude extract was purified using a Bio-Rad Profinity IMAC Ni-Charged Resin (Hercules, CA) (Wang et al., 2011).

Two other recombinant proteins, polyphosphate glucokinase from *Thermobifida fusca* YX (TfuPPGK, briefly named PPGK) (Liao et al., 2012) and 6-phosphogluconate dehydrogenase from *Moor-ella thermoacetica* (Mth6PGDH, briefly named 6PGDH) (Wang et al., 2011), were produced and purified as described previously.

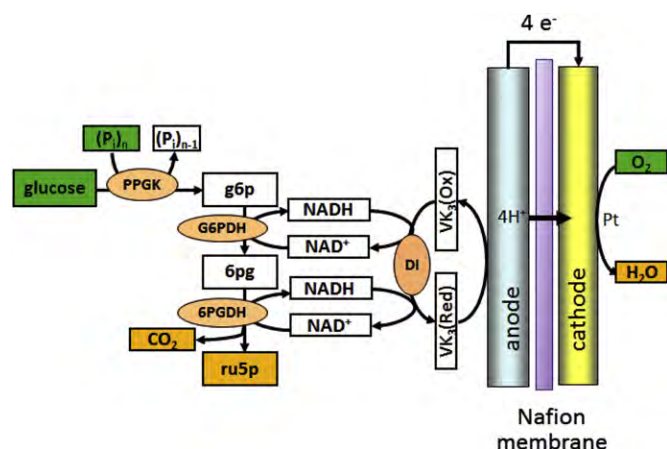


**Fig. 1.** Scheme of the synthetic enzymatic pathway for the deep oxidation of glucose without ATP in the enzymatic fuel cell. PPGK, polyphosphate glucokinase; G6PDH, glucose-6-phosphate dehydrogenase; 6PGDH, 6-phosphogluconate dehydrogenase; DI, diaphorase; g6p, glucose-6-phosphate; 6pg, 6-phosphogluconate; ru5p, ribulose-5-phosphate; and  $\text{VK}_3$ , vitamin  $\text{K}_3$ .

### 2.3. Enzyme activity assays

The activities of PPGK and 6PGDH were assayed at 23 °C (room temperature) as described previously (Liao et al., 2012; Wang et al., 2011). The activity of G6PDH was assayed in 50 mM HEPES buffer, 100 mM NaCl, 2.5 mM glucose-6-phosphate (G6P), 2.5 mM NAD<sup>+</sup>, 5 mM MgCl<sub>2</sub>, and 0.5 mM MnCl<sub>2</sub> at 23 °C. An increase in the absorbance at 340 nm due to the formation of NADH was measured using a UV spectrometer (Wang et al., 2011). The activity of DI was tested in 10 mM phosphate buffered saline buffer, 0.16 mM NADH, and 0.1 mM dichlorophenolindophenol (DCPIP) at 23 °C. A decrease in the absorbance at 600 nm due to the consumption of DCPIP was measured using a photospectrometer (Chakraborty et al., 2008). The DI used in this study was the recombinant GsDI, whose specific activity was much higher than that of the Sigma-Aldrich DI at both room and elevated temperatures (data not shown).

### 2.4. Bioanode fabrication

Dehydrogenase was immobilized on the anode by the electrostatic force as described previously (Zhu et al., 2011). The carbon paper electrode was cut into an “L” shape and activated in a 2.5% K<sub>2</sub>Cr<sub>2</sub>O<sub>7</sub> solution containing 10% HNO<sub>3</sub> by scanning it at 5 mV s<sup>-1</sup> from 1.55 V to 1.75 V versus a standard silver chloride electrode followed by a rinse with water. 10 μL of a 2% PLL solution, 10 μL of a G6PDH solution (0.4 U μL<sup>-1</sup>), 10 μL of a DI solution (1 U μL<sup>-1</sup>), 10 μL of a VK<sub>3</sub> solution (0.29 M in acetone), and 10 μL of a PAAcNa solution (0.066%) were placed onto a 1 cm<sup>2</sup> piece of carbon paper. Drying was conducted at room temperature after each reagent was added. In this study, recombinant GsDI was always used. The G6PDH used for immobilization was either one from Sigma-Aldrich or recombinant GsG6PDH. For a two-enzyme immobilization on the anode, forty μL of 6PGDH solution (0.08 U μL<sup>-1</sup>) was added after G6PDH immobilization. The bioanodes were stored in 100 mM HEPES buffer containing 2 mM NADH and 100 mM NaNO<sub>3</sub> at 4 °C before use.

### 2.5. Conditions of electrochemical measurements

The setup of the tested enzymatic fuel cells is shown in Fig. 2. Nafion 112 was used to separate the anode and cathode. The carbon cloth cathode was coated with 0.5 mg cm<sup>-2</sup> Pt as the catalyst. The general anolyte solution was 100 mM HEPES buffer (pH 7.2) containing 2 mM NAD<sup>+</sup>, 20 mM Mg<sup>2+</sup>, 0.5 mM Mn<sup>2+</sup>, 10 mM glucose, and 2 mM polyphosphate (34 mM phosphate unit equivalents). The enzyme-wired bioanodes were dipped into the solution, and the reaction solution was stirred at a rate of 600 rpm at 23 °C unless stated otherwise. The reaction solution was freshly prepared. For the PPGK loading optimization experiments, 1, 2, 3,

or 5 U of PPGK was added at 10 mM glucose. At a fixed ratio of 5 U of PPGK per 10 mM glucose, the glucose concentration was changed from 3 to 30 mM to study the electrochemical performance of the EFCs with bioanodes that contained both G6PDH and 6PGDH for the deep oxidation of glucose. To compare the performance of the bioanodes containing recombinant thermo-enzymes and/or Sigma-Aldrich LmG6PDH, the following reaction temperatures were tested: 23, 37, 50 and 70 °C. For all of the experiments, open circuit potential and linear sweep voltammetry were performed at a scan rate of 1 mV s<sup>-1</sup> using a CHI1000B Series Multi-Channel Potentiostat from CH Instruments, Inc. (Austin, TX) as described previously (Zhu et al., 2011). Polarization curves were recorded and power curves were generated by a computer equipped with the vendor's software. All experiments were performed in triplicate.

### 2.6. Determination of ribulose 5-phosphate

The final product of two-enzyme EFCs was ribulose-5-phosphate, which was assayed by a modified Dische's cysteine-carbazole method (Sun et al., 2012). After 4 h running, 100 μL of the electrolyte of the EFC was mixed with 1 mL of 66% H<sub>2</sub>SO<sub>4</sub>, 35 μL of 0.12% carbazole dissolved in ethanol and 35 μL of 1.5% cysteinium chloride. The mixture was incubated at 37 °C for 30 min and the absorbance at 540 nm was measured for quantifying ribulose-5-phosphate formed (Sun et al., 2012).

## 3. Results and discussion

### 3.1. A novel synthetic enzymatic pathway

Different from the direct oxidation of glucose by glucose oxidase or glucose dehydrogenase (Gao et al., 2010; Sakai et al., 2009; Zebda et al., 2011), glucose-6-phosphate (G6P) was chosen as a precursor in the EFCs because enzymes usually work more rapidly on phosphate-activated sugars than on their non-phosphate-activated counterparts (Moehlenbrock et al., 2011; Yoon et al., 2009). To avoid using costly ATP for the activation of glucose (Moehlenbrock et al., 2011; Zhu et al., 2011), glucose was phosphorylated to G6P by a newly discovered polyphosphate glucokinase (PPGK) from *T. fusca* in the presence of low-cost, stable polyphosphate in the aqueous phase (Liao et al., 2012). Furthermore, immobilized G6PDH was responsible for converting G6P to 6-phosphogluconate (6PG) and 6PGDH was responsible for converting 6PG to ribulose-5-phosphate and releasing one CO<sub>2</sub>. As a result, a cascade of two dehydrogenases enabled the generation of two mol of nicotinamide adenine dinucleotide (NADH) per mol of G6P. Two mol of NADH can be converted into NAD<sup>+</sup> through diaphorase (DI) and vitamin K<sub>3</sub> (VK<sub>3</sub>) to the cathode (Fig. 1). This pathway demonstrated the deeper oxidation of glucose using two cascade dehydrogenases.

In nature, most organisms utilize hexokinase to generate G6P at the cost of one ATP consumed per glucose, and then G6P enters hexose metabolic pathways (e.g., glycolysis and pentose phosphate pathways) (Ralph et al., 2008) because organisms have ATP regeneration systems. However, it is too costly to continuously supply ATP in *in vitro* biological systems (Zhang et al., 2011). For the proof-of-concept experiment, it was feasible to generate G6P for the EFC (Moehlenbrock et al., 2011), but it may be economically prohibitive for practical applications because of the high cost and instability of ATP.

In the natural pentose phosphate pathway, G6PDH and 6PGDH prefer to generate NADPH, which is used in anabolism, rather than NADH, which is used in catabolism; however, NADPH was not as effective as NADH in electron transfer to the bioanode

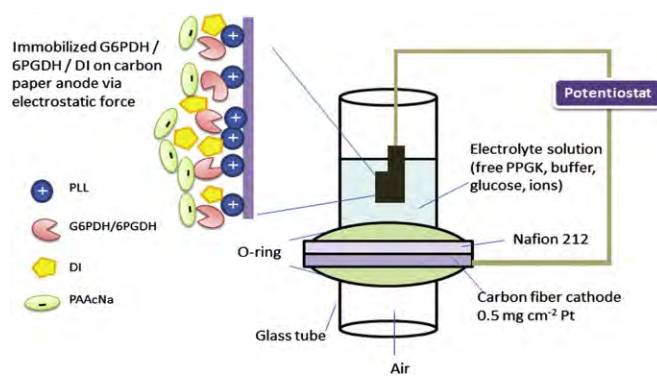


Fig. 2. Scheme of enzyme immobilization and the “I-cell” EFC setup for this study.

**Table 1**Summary of recombinant thermoenzymes produced in *E. coli*.

Thermoenzyme	EC	GeneBank #	Purification <sup>a</sup>	Sp. Act. <sup>b</sup> (U/mg)
Polyphosphate glucokinase (TfuPPGK)	2.7.1.63	YP289867	CBM	7.8 ± 0.3
Glucose-6-phosphate dehydrogenase (GsG6PDH)	1.1.1.49	JQ040549	His/NTA	1.1 ± 0.1
6-phosphogluconate dehydrogenase (Mth6PGDH)	1.1.1.44	ABC19597	His/NTA	5.1 ± 0.2
Diaphorase (GsDI)	1.6.99.3	JQ040550	His/NTA	188 ± 10

<sup>a</sup> CBM: Cellulose binding module-tagged purification method (Liao et al., 2012); His/NTA: His-tagged protein binding on nickel resin (Wang et al., 2011).<sup>b</sup> Sp. act., specific activity, which was measured as described in materials and methods.

(Zhang et al., 2011). Therefore, for the pathway that we designed, we screened numerous thermophilic G6PDHs and 6PGDHs found in the literature and characterized putative G6PDHs and 6PGDHs from the expanding genomic DNA databases of thermophiles. Finally, we discovered a G6PDH and 6PGDH that prefer to generate NADH: G6PDH from *G. stearothermophilus* and 6PGDH from *M. thermoacetica*. Table 1 presents the basic information about the recombinant thermoenzymes that were used in this study: PfuPPGK, GsG6PDH, Mth6PGDH and GsDI. All four recombinant thermoenzymes were purified to homogeneity and examined by SDS-PAGE (data not shown). The specific activities of GsG6PDH and Mth6PGDH were  $1.1 \pm 0.1$  and  $5.1 \pm 0.2$  U mg<sup>-1</sup> at room temperature, respectively.

### 3.2. Optimization of PPGK loading

To perform the PPGK-mediated generation of G6P from glucose, the loading of PPGK was optimized at 10 mM glucose (Fig. 3). When PPGK loading was increased from 1 to 5 U per 10 mM of glucose, the maximum power density increased from 0.0045 to 0.0154 mW cm<sup>-2</sup> in the G6PDH-only EFC. There were small differences between the power and current densities in the cases of 3 and 5 U of PPGK, suggesting that 5 U of PPGK per 10 mM of glucose was sufficient. Therefore, 5 U of PPGK per 10 mM of glucose was chosen for use in subsequent experiments.

### 3.3. Deep oxidation of glucose through two dehydrogenases

The performance of two EFCs containing 4 units of GsG6PDH and 4 units of GsG6PDH/3.2 U of Mth6PGDH was examined at glucose concentrations ranging from 3 to 30 mM (Fig. 4). The EFC containing co-immobilized GsG6PDH and Mth6PGDH always showed higher power and current densities than the EFC containing only immobilized G6PDH. The maximum power densities of EFCs containing only G6PDH were 0.0061, 0.0154, and 0.0224 mW cm<sup>-2</sup> at glucose concentrations of 3 mM, 10 mM, and 30 mM, respectively. By contrast, the power densities of EFCs containing both G6PDH and 6PGDH were 0.0095, 0.0203, and 0.0252 mW cm<sup>-2</sup>. Clearly, the EFC containing two dehydrogenases exhibited higher power and current densities than the EFC containing one dehydrogenase regardless of the substrate concentration. The final product of ribulose-5-phosphate generated by two dehydrogenase-based EFC was examined. Approximately 0.1 mM of ribulose-5-phosphate was generated in the solution after 4 h running based on 10 mM of glucose. These results suggest that the deep oxidation of glucose was achieved by using a cascade of two dehydrogenases.

Nearly all glucose-powered EFCs are based on the utilization of a single redox enzyme in the bioanode to generate two electrons per glucose (Coman et al., 2010; Gao et al., 2009; Sato et al., 2005). In principle, one mole of glucose can generate 24 electrons through its complete oxidation. In this study, four electrons were generated from glucose by using two dehydrogenases, resulting in a doubling of the energy extraction potential from glucose compared to one redox enzyme-based glucose enzymatic fuel cells; in the future, it could be converted to G6P through the non-oxidative pentose

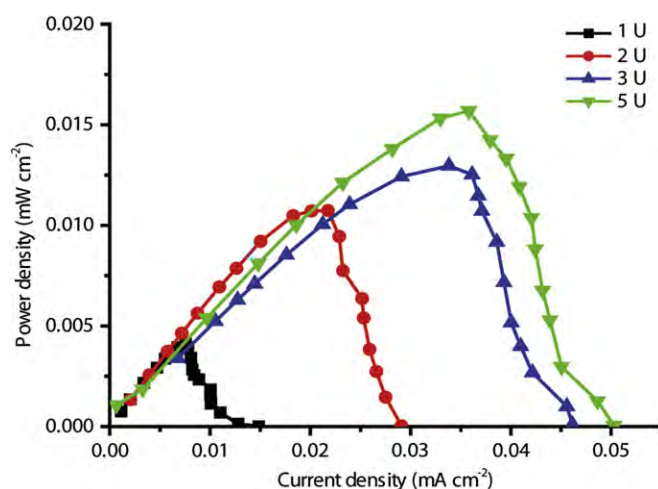


**Fig. 3.** Profiles of the power densities versus the current densities of the GsG6PDH-based EFC at PPGK loadings of 1, 2, 3, and 5 units at 10 mM glucose.

phosphate pathway. To completely oxidize glucose, a pathway based on glycolysis and the TCA cycle containing more than 20 enzymatic steps was hypothesized so that 24 electrons could be generated (Sokic-Lazic et al., 2010), but the proof-of-concept experiment has not yet been published. This hypothetical pathway might be difficult to use in practical applications because it would require costly ATP as input and would involve highly labile coenzymes such as CoA. Recently, Xu and Minteer (2011) demonstrated the use of a six-enzyme pathway in the anode for the deep oxidation of glucose; however, its maximum power density remained very low (0.0065 mW cm<sup>-2</sup>), which is much lower than the maximum power densities that we achieved (0.020 mW cm<sup>-2</sup> at room temperature and 0.322 mW cm<sup>-2</sup> at 50 °C).

### 3.4. High power output at elevated temperatures

The use of thermoenzymes in EFCs could have three benefits: prolonged enzyme lifetime, high power output at elevated temperatures, and a broad working temperature range. The performance of the two dehydrogenase-based EFCs containing the recombinant GsG6PDH and the Sigma-Aldrich mesophilic G6PDH, which originated from *L. mesenteroides* (LmG6PDH), was compared at 10 mM glucose and at 23 °C, 37 °C, 50 °C, and 70 °C (Fig. 5). At 23 °C, it was found that both EFCs exhibited similar power outputs regardless of the enzyme source. Both EFCs had higher power densities at 37 °C and 50 °C than those at 23 °C. For the mesophilic enzyme-based EFC, a maximum power density of  $0.059 \pm 0.003$  mW cm<sup>-2</sup> was obtained at 37 °C. A remarkable increase in the maximum power density of the thermoenzyme-based EFC occurred at 50 °C; it reached a maximum power density of  $0.322 \pm 0.017$  mW cm<sup>-2</sup> at 50 °C. This value was approximately 8-fold more than the power density of the EFC containing the mesophilic LmG6PDH. When the temperature was

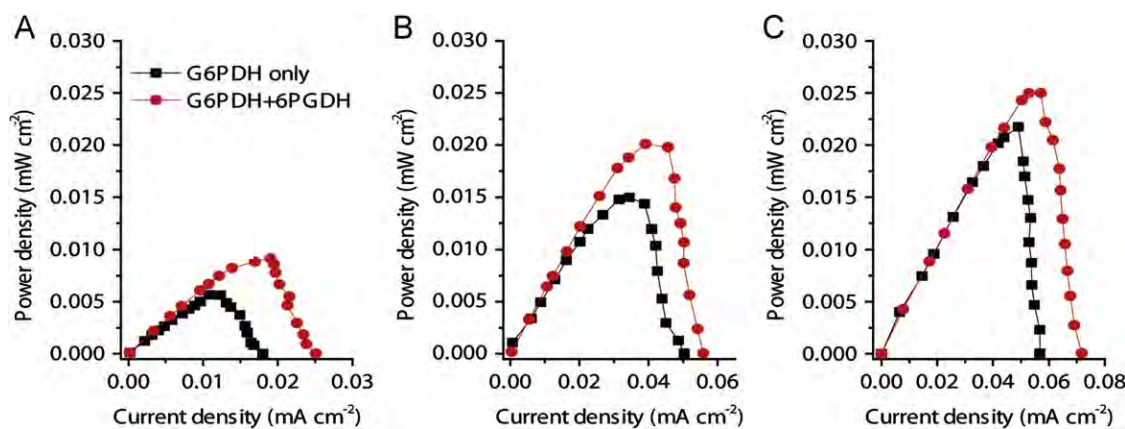


Fig. 4. Profiles of the power densities versus the current densities of the GsG6PDH-based and the GsG6PDH/Mth6PGDH-based EFCs at glucose concentrations of 3 mM (A), 10 mM (B), and 30 mM (C).

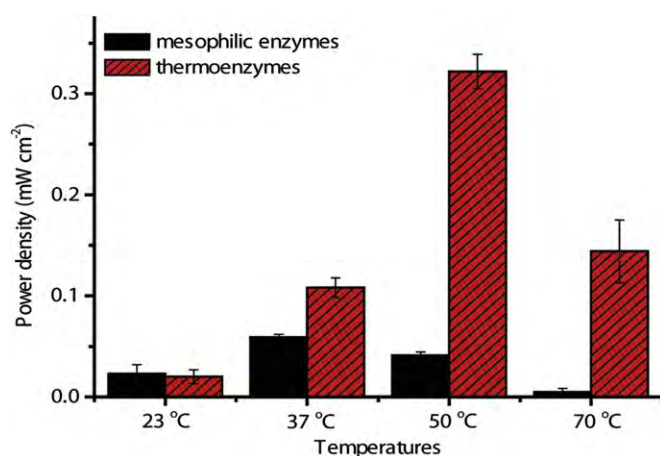


Fig. 5. Comparison of the maximum current densities of the GsG6PDH/Mth6PGDH-based EFC (thermoenzyme) and the LmG6PDH/Mth6PGDH-based EFC (mesophilic enzyme) at 23, 50 and 70 °C.

increased to 70 °C, both EFCs had much lower power outputs than at 50 °C. It was noted that the mesophilic enzyme-based EFC had a very low output density compared to its output densities at 23 °C and 50 °C because of the fast deactivation of the enzyme at 70 °C.

The thermoenzyme-based EFC exhibited a maximum power density of  $0.322 \pm 0.017$  mW cm<sup>-2</sup> at 50 °C, which was approximately 15.8 times higher than that at 23 °C ( $0.020 \pm 0.007$  mW cm<sup>-2</sup>). The much higher power density at the elevated temperature was attributed to the following factors: (i) the higher activity of thermoenzymes (Wang and Zhang, 2009) and (ii) the better mass transfer at elevated temperature (Fogler, 1999). The use of thermoenzymes in EFCs would allow them to work over a broad temperature range, especially in high temperature areas such as tropical areas, deserts, and closed, small rooms containing heat-releasing devices.

#### 4. Conclusions

A new enzymatic pathway to generate electricity from glucose in EFCs containing PPGK, G6PDH and 6PGDH has been demonstrated. The deep oxidation of glucose through a cascade of two dehydrogenases means the potential to double the energy storage density compared with the oxidation of glucose through one dehydrogenase or oxidase. The use of thermoenzymes enabled

markedly increased power outputs at elevated temperatures, suggesting that running thermoenzyme-based EFCs at high temperatures is feasible.

#### Acknowledgments

This work was supported mainly by the Air Force Office of Scientific Research MURI grant (FA9550-08-1-0145), and partially by DOE Bioenergy Science Center (BESC) and CALS Bioprocessing and Biodesign Center.

#### References

- Akers, N.L., Moore, C.M., Minteer, S.D., 2005. *Electrochimica Acta* 50 (12), 2521–2525.
- Archederra, R.L., Treu, B.L., Minteer, S.D., 2007. *Journal of Power Sources* 173 (1), 156–161.
- Chakraborty, S., Sakka, M., Kimura, T., Sakka, K., 2008. *Bioscience, Biotechnology, and Biochemistry* 72, 877–879.
- Coman, V., Ludwig, R., Harreither, W., Haltrich, D., Gorton, L., Ruzgas, T., Shleev, S., 2010. *Fuel Cells* 10 (1), 9–16.
- Cooney, M.J., Svoboda, V., Lau, C., Martin, G., Minteer, S.D., 2008. *Energy and Environmental Science* 1 (3), 320–337.
- Davis, F., Higson, S.P.J., 2007. *Biosensors and Bioelectronics* 22 (7), 1224–1235.
- Fogler, H.S., 1999. *Elements of Chemical Reaction Engineering*. Prentice Hall PTR, Upper Saddle River, NJ.
- Gao, F., Courjean, O., Mano, N., 2009. *Biosensors and Bioelectronics* 25 (2), 356–361.
- Gao, F., Viry, L., Maugey, M., Poulin, P., Mano, N., 2010. *Nature Communications* 1 (2).
- Güven, G., Prodanovic, R., Schwaneberg, U., 2010. *Electroanalysis* 22 (7–8), 765–775.
- Liao, H.H., Myung, S., Zhang, Y.-H.P., 2012. *Applied Microbiology and Biotechnology* 93, 1109–1117.
- Minteer, S.D., Liaw, B.Y., Cooney, M.J., 2007. *Current Opinion in Biotechnology* 18 (3), 228–234.
- Moehlenbrock, M., Minteer, S., 2008. *Chemical Society Reviews* 37, 1188–1196.
- Moehlenbrock, M.J., Meredith, M.T., Minteer, S.D., 2011. *ACS Catalysis* 1, 17–25.
- Osman, M.H., Shah, A.A., Walsh, F.C., 2011. *Biosensors and Bioelectronics* 26 (7), 3087–3102.
- Palmore, G.T.R., Bertschy, H., Bergens, S.H., Whitesides, G.M., 1998. *Journal of Electroanalytical Chemistry* 443 (1), 155–161.
- Ralph, E.C., Thomson, J., Almaden, J., Sun, S.X., 2008. *Biochemistry-Us* 47 (17), 5028–5036.
- Rubenwolf, S., Kerzenmacher, S., Zengerle, R., von Stetten, F., 2011. *Applied Microbiology and Biotechnology* 89 (5), 1315–1322.
- Sakai, H., Nakagawa, T., Tokita, Y., Hatazawa, T., Ikeda, T., Tsujimura, S., Kano, K., 2009. *Energy and Environmental Science* 2, 133–138.
- Sato, F., Togo, M., Islam, M.K., Matsue, T., Kosuge, J., Fukasaku, N., Kurosawa, S., Nishizawa, M., 2005. *Electrochemistry Communications* 7 (7), 643–647.
- Sokic-Lazic, D., Archederra, R.L., Treu, B.L., Minteer, S.D., 2010. *Electroanalysis* 22 (7–8), 757–764.
- Sokic-Lazic, D., Minteer, S.D., 2009. *Electrochemical and Solid-State Letters* 12 (9), F26–F28.
- Sun, F.F., Zhang, X.Z., Myung, S., Zhang, Y.-H.P., 2012. *Protein Expression and Purification* 82, 302–307.

- Wang, Y., Huang, W., Sathitsuksanoh, N., Zhu, Z., Zhang, Y.-H.P., 2011. *Chemistry and Biology* 18, 372–380.
- Wang, Y., Zhang, Y.-H.P., 2009. *Microbial Cell Factories* 8, 30.
- Xu, S., Minteer, S.D., 2011. *ACS Catalysis* 1, 91–94.
- Yoon, R.-Y., Yeom, S.-J., Kim, H.-J., Oh, D.-K., 2009. *Journal of Biotechnology* 139 (1), 26–32.
- You, C., Zhang, X.-Z., Zhang, Y.-H.P., 2012. *Applied and Environmental Microbiology* 78, 1593–1595.
- Zebda, A., Gondran, C., Le Goff, A., Holzinger, M., Cinquin, P., Cosnier, S., 2011. *Nature Communications* 2, 370.
- Zhang, Y.-H.P., 2010. *Biotechnology and Bioengineering* 105, 663–677.
- Zhang, Y.-H.P., 2011. *Proceedings of Biochemistry* 46, 2091–2110.
- Zhang, Y.-H.P., Myung, S., You, C., Zhu, Z.G., Rollin, J., 2011. *Journal of Materials Chemistry* 21 (47), 18877–18886.
- Zhu, Z., Wang, Y., Minteer, S., Zhang, Y.-H.P., 2011. *Journal of Power Sources* 196, 7505–7509.